Jour. of the KGS, Vol. 23, No. 3. March 2007, pp. 123~131

Relationship between the State Parameter and Cone Resistance of Busan Sand

부산모래의 상태정수와 콘저항치 상관관계

Kim, Seung-Han[1] 김 승 한 Lee, Moon-Joo[1] 이 문 주
Choi, Sung-Kun[1] 최 성 근 Hong, Sung-Jin[1] 홍 성 진
Lee, Woo-Jin[2] 이 우 진

요 지

일련의 CID 삼축압축시험과 실내콘관입시험을 통하여 부산모래에서의 상태정수와 정규화된 콘저항치의 상관관계를 파악하였다. 삼축압축시험결과를 토대로 부산모래의 한계상태선을 도출하였으며 3개의 한계상태정수는 $M = 1.39$ ($\phi_{cs} = 34°$), $\Gamma = 1.07$ 및 $\lambda = 0.068$인 것으로 산출되었다. 부산모래의 상태정수와 정규화된 콘저항치의 상관관계는 $(q_c - p)/p' = 27.6 \exp(-10.9\psi)$의 식으로 표현되었으며, 이는 응력이력에 관계없이 동일함을 확인하였다. 문헌조사를 통해 얻은 다른 모래시료의 정규화된 콘저항치 기울기 m 및 $\psi = 0$ 에서의 절편값 κ를 비교 분석한 결과, 부산모래는 유사한 λ_{ss} 값을 갖는 모래시료 중 가장 큰 κ 값을 보였으나, m과 κ가 λ_{ss}와 갖는 관계는 기존에 발표된 자료와 일치함을 확인하였다.

Abstract

A series of CIDC triaxial tests and cone penetration tests in calibration chamber were performed to investigate the relationship between state parameter and normalized cone resistance for dredged Busan sand. From the results of the triaxial tests, the critical state line of Busan sand was established, and the critical state parameters found to be $M = 1.39$ ($\phi_{cs} = 34°$), $\Gamma = 1.07$ and $\lambda = 0.068$. By analyzing the state parameters and corresponding cone resistances for calibration chamber specimens, the relationship between normalized cone resistance and state parameter for Busan sand was defined as $(q_c - p)/p' = 27.6 \exp(-10.9\psi)$. This relationship was also shown to be independent of the stress history. From the comparison of the slope of the normalized cone resistance, m, and the normalized cone resistance at $\psi = 0$, κ, with those of various sandy soils from over the world, the relationship of m and κ with λ_{ss} of Busan sand was concluded to show a good agreement with the result published previously, while Busan sand had the largest κ among the soils with similar λ_{ss} values.

Keywords : Busan sand, Calibration chamber, Cone resistance, Critical state, Shear response, State parameter

1. Introduction

Korea, as well as other neighboring countries, has invested both public and private funds for the construction of a number of harbors and airports in order to facilitate transportation and preoccupy international logistics service market. In Korea, Busan new port is under construction with the aim of serving as a gateway hub for the Northeast

1 Member, Graduate Student, Dept. of Civil and Environmental Engineering, Korea Univ., Seoul
2 Member, Associate Professor, Dept. of Civil and Environmental Engineering, Korea Univ., Seoul, woojin@korea.ac.kr, Corresponding Author

Asia. A large amount of sand was dredged from the offshore seabed for reclamation. Hence, investigating the shear behavior of Busan sand deserves academic attention.

The behavior of sandy soil subjected to drained shear can be contractive, intermediate, or dilative. For a dilative specimen, the void ratio decreases to a minimum transient value, known as the characteristic state (Luong, 1980), prior to the peak strength and then increases again until its void ratio reaches the critical state. For a contractive specimen, the void ratio continuously decreases toward the void ratio at the critical state. The critical state is defined as the ultimate state at which the soil continues to deform with a constant stress and void ratio. The response of a specimen can be captured in 3-D space in terms of the void ratio (e), mean principal stress ($p' = (\sigma_1' + 2\sigma_3')$), and deviator stress ($q = (\sigma_1 - \sigma_3)$). For simplicity, the projections of the critical state line in two planes ($p' - q$ and e-log p' plane) are commonly used, where three critical state parameters are able to be determined. The slope of the critical state line in the $p' - q$ plane is expressed in terms of the critical state friction angle, ϕ_{cs}.

$$M = \left(\frac{q}{p'}\right)_{cs} = \frac{6\sin\phi_{cs}}{3-\sin\phi_{cs}} \tag{1}$$

The critical state line projected in the semi-logarithmic e-log p' plane is expressed in terms of the intercept, Γ, and slope, λ.

$$e_{cs} = \Gamma - \lambda \log\left(\frac{\sigma'_{cs}}{1kPa}\right) \tag{2}$$

The critical state line stands for a reference state affected by various physical properties of a sandy soil, such as the compressibility, internal friction angle, grain size distribution and shape, mineralogy, and extreme void ratios. Theoretically, the critical state line represents a condition of zero volume change during shear (Poulos, 1981). The shear behavior of a sandy soil can be either contractive or dilative depending on whether the initial void ratio is greater or lesser than the void ratio of the critical state. Actually, the further a material state is from the critical state condition, the stronger will be the tendency for a volume change during shear. Quantification of this tendency for a specimen to change its volume is achievable using the concept of state parameter (ψ).

The two most influential factors affecting the behavior of a given soil are the void ratio and stress level. The state parameter combines the influence of both of these factors, and can be used to describe the shear behavior of a sandy soil. The state parameter is defined as the difference between the void ratio of a soil and the void ratio on the ultimate (steady or critical) state line at the same mean effective stress, as illustrated in Fig. 1. Actually, despite of some controversy, the ultimate state of a soil has been reported to be independent of the initial stress state (Ishihara, 1993, Vaid and Thomas, 1995, Chu, 1995), initial fabric (DeGregorio, 1990, Ishihara, 1993), loading condition (DeGregorio, 1990, Been et al., 1991), and drainage condition (Been et al, 1991, Chu, 1995), even though the shear response and quasi-steady state may differ. In this study, therefore, the critical state line was assumed to be identical to the steady state line.

Finding the relationship between the cone resistance and state parameter is initiated based on the fact that the small strain behavior, such as shear modulus or compressibility, does not correlate well with the state parameter; whereas, the correlation between the state parameter and the large strain behavior, such as drained angle of shearing resistance, is considered acceptable. Been et al. (1986) provided a better relationship between the cone resistance and state parameter for a sandy soil using data collected from available chamber testing programs. Concluding that the relationship relies on the characteristics of the soil,

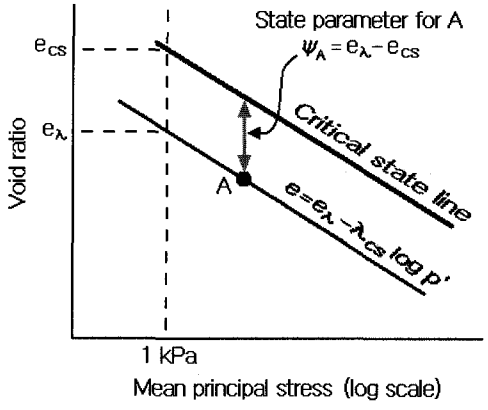

Fig. 1. Definition of state parameter ψ

Been et al. (1986) suggested the following correlation in terms of the slope, m, and the intercept, κ.

$$\frac{q_c - p}{p'} = \kappa \exp(-m\psi) \tag{3}$$

In this paper, the critical state of Busan sand was determined using a series of conventional CIDC tests, and then the chamber cone tests data were correlated with the state parameter. Also, the gradient and intercept of the q_c - Ψ relationship of Busan sand were evaluated and compared with other values published previously.

2. Experimental Program

2.1 Property of Busan Sand

Busan sand is natural soil dredged near Yokji Island in the South Sea. Its properties are summarized in Table 1. The basic properties were evaluated using standardized techniques, KSF2308 (specific weight), KSF2302 (sieve analysis), and DIN18126 (extreme void ratios). The particle size distribution and SEM images are shown in Fig. 2. Distinguished characteristics of Busan sand are its high content of crushed shell.

2.2 CIDC Test

The specimen for the triaxial test had a diameter of 70.6 mm and height of 156.0 mm. Porous stones with a Norton mixture number of P260 were used with a sheet of filter paper at the top and bottom plates. In this paper, eighteen drained shear tests were performed with different relative densities and confining pressures. The complete CIDC triaxial test program is summarized in Table 2.

Dense and medium specimens were formed using the air-pluviation method. For loose and very loose specimens, both the air-pluviated and moist-tamped specimens were tested to monitor the differences in the shear behavior. Moist-tamping is considered adequate for preparation of a loose specimen close to the maximum void ratio; whereas, the air-pluviated loose specimen shows dilative behavior, regardless of its void ratio (Been and Jefferies, 1985). For air-pluviation, a funnel and a diffuser are required to prevent material segregation and to regulate the soil deposition rate and energy, which determine the resulting density. The drop heights of the air-pluviation system are predetermined according to the densities. For moist-tamping, soils are mixed to have moist content of 5%, and then placed in ten layers to the predetermined height of a mold. This procedure has to be performed with great caution to enhance the homogeneity. Before the mold was disassembled, the specimen was held with a vacuum pressure of 35 kPa (5 psi) constantly maintained using a regulator. Saturation was achieved in three phases; firstly, specimen was flushed with carbonate water, then

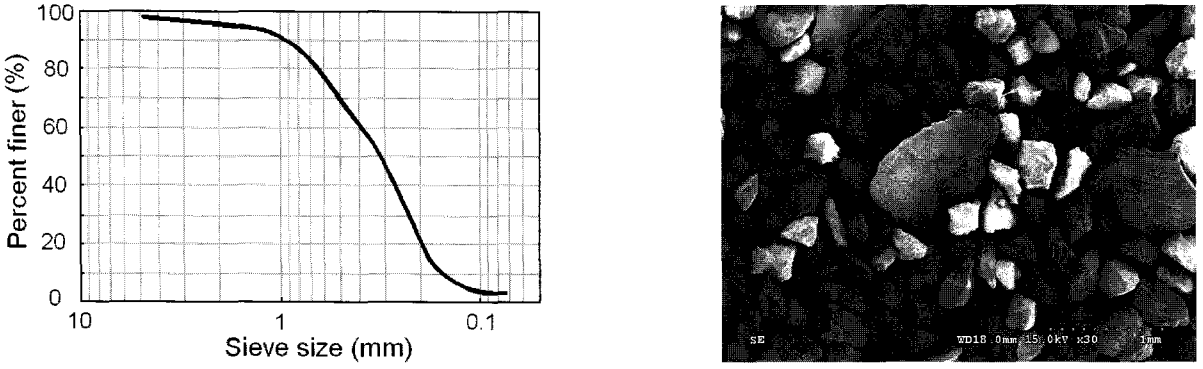

(a) Particle size distribution (b) SEM image

Fig. 2. Particle size distribution and a microphotograph

Table 1. Properties of Busan sand

G_S	e_{max} (γ_{dmin})	e_{min} (γ_{dmax})	D_{50} (mm)	D_{10} (mm)	C_u	C_c	Particle Shape	Mineralogy (%)
2.62	1.063(1.27)	0.658(1.58)	0.315	0.162	0.71	2.35	Angular to sub-angular	SiO_4(84.69), $CaCO_3$(7.25)

Table 2. CIDC test program

Confinement	Moist tamping		Air-Pluviation			
	20%	40%	20%	40%	60%	80%
100 kPa	M21	M41	A21	A41	A61	A81
200 kPa	M22	M42	A22	A42	A62	A82
400 kPa	M24	M44	A24	A44	A64	A84

saturated using de-aerated water. Because of the high solubility of carbon dioxide in water, rapid and complete saturation is insured; back-pressure was finally applied until B value of at least 0.97 was achieved. The same value of back-pressure (100 kPa) was applied for all specimens. With increment of 50 kPa per two minutes, the isotropic consolidation pressure was applied to the target effective confining pressure. After the completion of the isotropic consolidation, the strain-controlled shear tests were performed with a 0.5%/min strain rate until an axial strain of 30% was reached. Time, axial strain, volumetric strain, deviatoric stress, and total and effective confining stresses were recorded every 1 second using an automatic data acquisition system.

2.3 Chamber Cone Penetration Test

The Korea University Calibration Chamber System (KUCCS) was devised to simulate in-situ tests under various boundary conditions and stress states. The system consists of a calibration chamber, control panel, and data acquisition system. The calibration chamber, 1.2 and 1.0 meters in diameter and height, respectively, is capable of performing K_0 consolidation, using a servo-controlled double wall and piston underneath the base-plate (Fig. 3), as well as consolidation following arbitrary stress path under four boundary conditions. Chamber cone penetration test is able to be conducted using cone-probe adapters located on the top plate.

As the chamber-to-cone diameter ratio and boundary condition are known to have a significant influence on the results of the cone penetration test, a number of correction methods have been suggested to account for the effects of the chamber size and boundary condition. In this paper, the chamber size standardization factors suggested by Been et al. (1986) were used, which defines the correction factors according to the boundary condition and chamber-to-cone diameter ratio based on the data of Hokksund sand. Although this standardization technique is based on limited test data, for the sake of consistency with previously published papers, the calibration chamber test results were corrected using this technique.

The chamber specimen was prepared using a large scale pluviation method. This technique was preferred due to its effectiveness, and repeatability in forming identical samples with spatial homogeneity. The KUCCS raining equipment, as shown in Fig. 4, consists of a storage chamber, lower and upper molds, and a diffuser sieve,

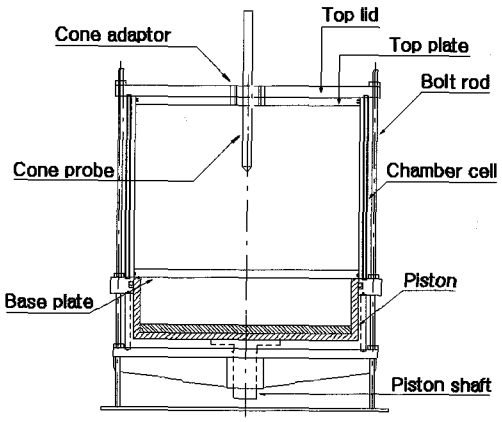

Fig. 3. Schematic of calibration chamber

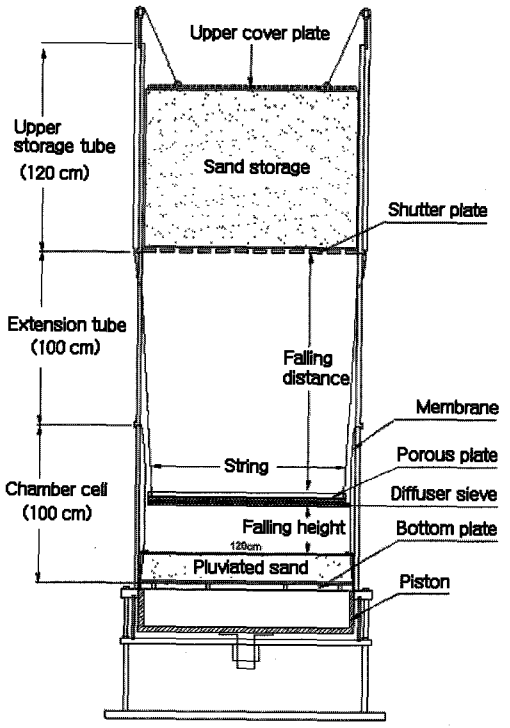

Fig. 4. Raining equipment

Table 3. Chamber cone penetration test program

Vertical confining pressure	Relative density		
	40%	60%	80%
100 kPa (OCR=1)	CN41	CN61	CN81
200 kPa (OCR=1)	CN42	CN62	CN82
400 kPa (OCR=1)	CN44	CN64	CN84
200 kPa (OCR=2)	CO42	CO62	CO82
100 kPa (OCR=4)	CO44	CO64	CO84
50 kPa (OCR=8)	CO48	CO68	CO88

which is capable of maintaining a constant drop height with the elevating diffuser sieve. The relative density of the specimen is governed by the opening size of the diffuser and the drop height, and these values were predetermined from a series of preliminary raining tests.

After assembling the spilt mold and rubber membrane, the specimen was pluviated using the raining system. The upper plate was mounted onto the specimen and was sealed with membrane and O-rings. Once the specimen was held with a vacuum pressure, the split mold was disassembled and the initial volume was measured. The double wall chamber cell, upper lid, and reinforcing plate were assembled and the inner and outer cells then completely filled with de-aerated water. The confining pressure was increased to a target value with increments of 50 kPa per every hour. By unloading from a vertical preconsolidation pressure of 400 kPa, the specimens with OCR of 2, 4 and 8 were prepared. The volume change in the specimen was measured by reading the water level in two vessels connected to the piston and chamber cell. Once the chamber specimen had stabilized at the desired consolidation pressure, the hydraulic thruster was located above the cone adapter on the reinforcing plate and cone probe is penetrated into the specimen at a standard penetration rate of 2 cm/sec. Eighteen cone penetration tests were performed according to the test program summarized in Table 3.

3. Experimental Results

3.1 Critical State Line of Busan Sand

Fig. 5 shows the results of the CIDC triaxial tests for Busan sand with different initial void ratios and effective confining pressures. Due to the dilating behavior of the air-pluviated specimen, Figs. 5 and 6a were plotted based on data acquired from the air-pluviated loose and medium specimens, as well as the moist-tamped dense and very dense specimens. From Fig. 5, as long as the confining pressures are the same, the shear strength of the soil converges to a certain residual value, regardless of the initial void ratio. The void ratios of the dense specimens, however, did not converge to the same value. The development of a shear band during shear may induce strain localization, which would affect the global void ratio. In addition to the strain localization effect, the end platen effect triggered by friction between the plates and the bordering soils plays a significant role in preventing the specimen from dilating, as a result, lowering the global void ratio. The transient void ratio, which is known to appear as a minimum void ratio prior to the peak strength in medium-dense or dense specimens, can be seen clearly with a specimen under a large confining pressure. It can be clearly observed in the specimen with 400 kPa confinement, whereas it is indistinguishable in the specimen with 100 kPa confinement. Figure 6b shows the difference between the shear responses of the moist-tamped samples and the air-pluviated samples. The air-pluviated samples turned out to be dilative even though the moist-tamped specimens at the same void ratio showed contractive behavior.

On the basis of the test data, including axial strain, void ratio, deviatoric stress, and confining stress at the critical

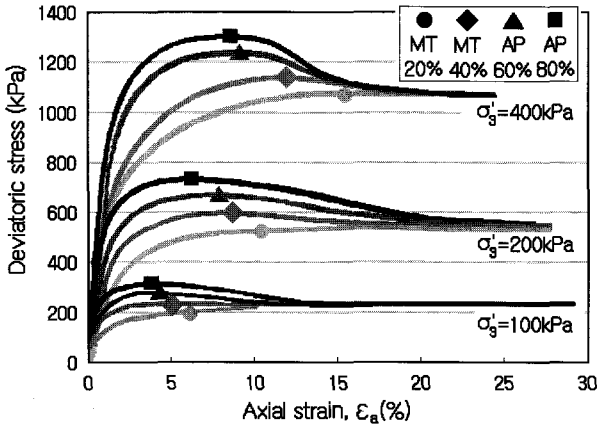

Fig. 5. Drained shear response

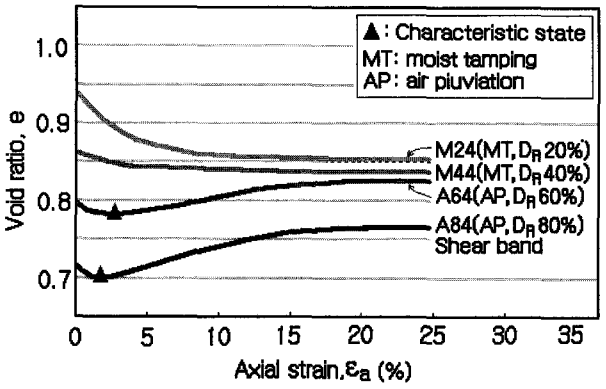

(a) Evaluation of critical void ratio

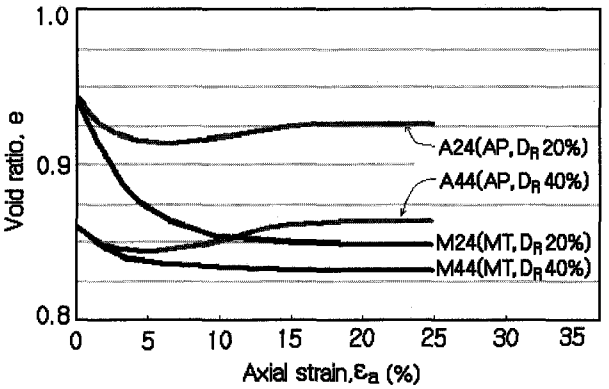

(b) Volumetric response for specimens formed by different methods

Fig. 6. Variation of void ratio with axial strain (σ'_3 = 400 kPa)

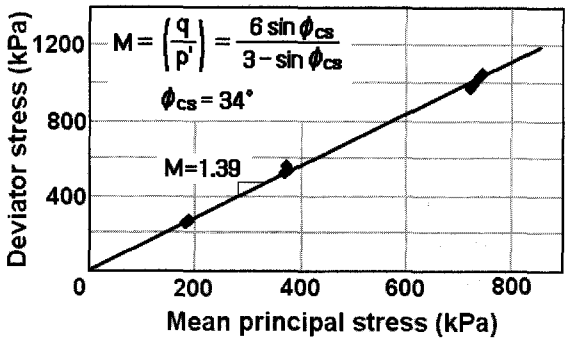

(a) CSL on p'-q plane

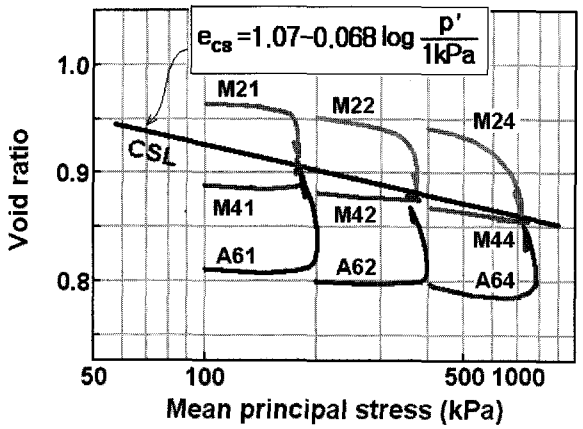

(b) CSL on e-log p' plane

Fig. 7. Critical state line for Busan sand

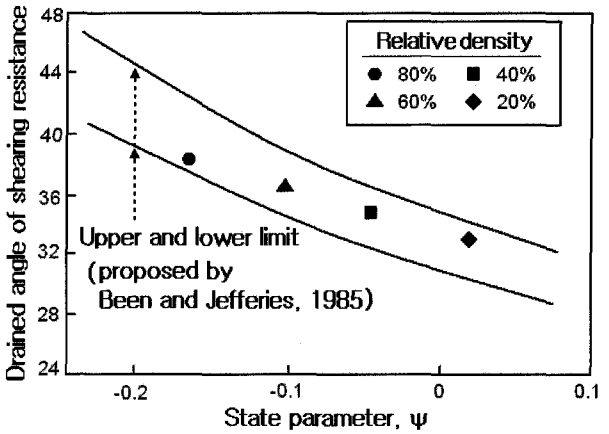

Fig. 8. Peak friction angle of Busan sand as a function of ψ

state, obtained from a series of CIDC tests, the critical state line and three parameters were determined, as illustrated in Fig. 7. It should be noted that, due to the insufficient void ratio convergence of the dense specimens, the shear responses of D_R = 80% specimens were excluded when determining the critical state line. The computed critical state parameters of Busan sand are M = 1.39, Γ = 1.07, and λ = 0.068. The friction angle at the critical state, ϕ_{cs}, was determined to be 34°, which is in good agreement with the typical value of ϕ_{cs} suggested by Bolton (1986), which was 33° for quartz sands.

Fig. 8 shows the relationship between the peak friction angle and state parameter for Busan sand. It was within the range proposed by Been and Jefferies (1985). Although the trends of decreasing ϕ'_{paek} with increasing ψ were quite similar, the gradient of the extreme limits was steeper than that for Busan sand. This indicates that the maximum dilation angle, ψ_{max}, of Busan sand is likely to be smaller than that of other sands, as reflected in the fact that the slope of the critical state line, which is basically a measure of the compressibility of soil, was relatively large for Busan sand.

3.2 Chamber Cone Penetration Test Result

The state parameters of the chamber specimens were calculated based on the void ratio after the completion of each K_0 consolidations. The representative cone resistance was determined as the value when the cone resistance measured during cone penetration into calibration chamber became constant. Also, the cone resistance was corrected using the chamber size standardization factor, and the normalized cone resistance wase obtained. From a series of preliminary raining tests, a 20% relative density was impossible to achieve and, as a result, data for $D_R = 20\%$ specimens was not obtained in the calibration chamber.

The points in Fig. 9 indicate the void ratio and stress state of each chamber specimen, all of which were below the critical state line. All the chamber specimens had negative state parameters, indicating a dilative shear response. The void ratio of the OC specimen was slightly smaller than that of the NC specimen due to the unrecoverable deformation during unloading. Fig. 10 shows the relationship between normalized cone resistance and the state parameter established for Busan sand. It is shown that the cone resistance increases as the density of the specimen increases, i.e. as the state parameter decreases. It was also observed that the linear regression lines of the NC and OC specimens show no discrepancy. Therefore, it can be concluded that the stress history does not affect the relationship between the cone resistance and state parameter when the cone resistance is normalized with respect to the mean effective normal stress. From the relationship, the values of m and for κ Busan sand were found to be 10.9 and 27.6, respectively.

Fig. 11 shows the contour lines determined by assigning specific numbers in place of the state parameter in Equation (3). The numbers in the figure represent the state parameter, e.g. 04 means ψ = -0.04. It was observed that the slope of the plot between $q_c - p$ and p' was closely related to the state parameter, and provided a good estimation for the state parameter of each chamber specimen.

Figs. 12a and 12b show the plots of the slope of the normalized cone resistance, m, and the normalized cone resistance at $\psi = 0$, κ, with respect to the slope of the steady state line, λ_{ss}, for various sandy soils from over the world. The data point for Busan sand is located at almost the same position with that of Reid Beddford in

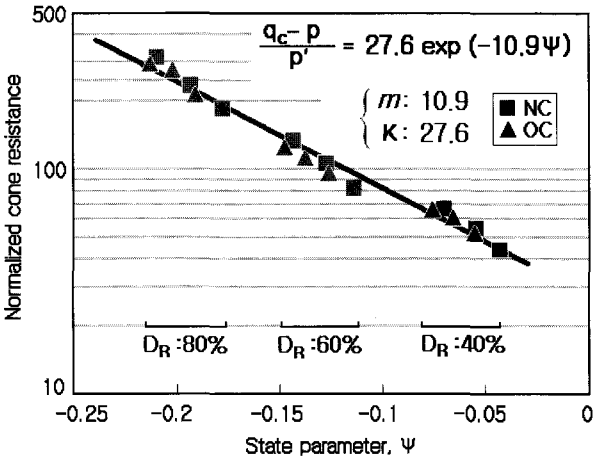

Fig. 10. Relationship between the state parameter and normalized cone resistance

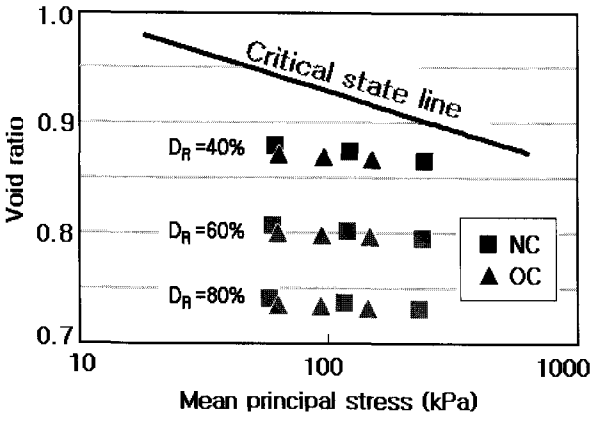

Fig. 9. State parameter for cone chamber specimen

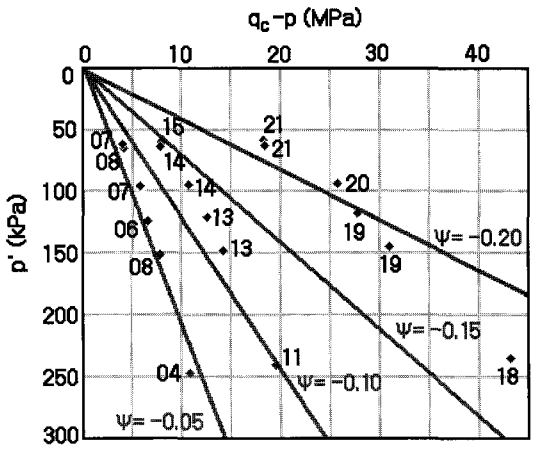

Fig. 11. Proportionality of the state parameter to the normalized cone resistance

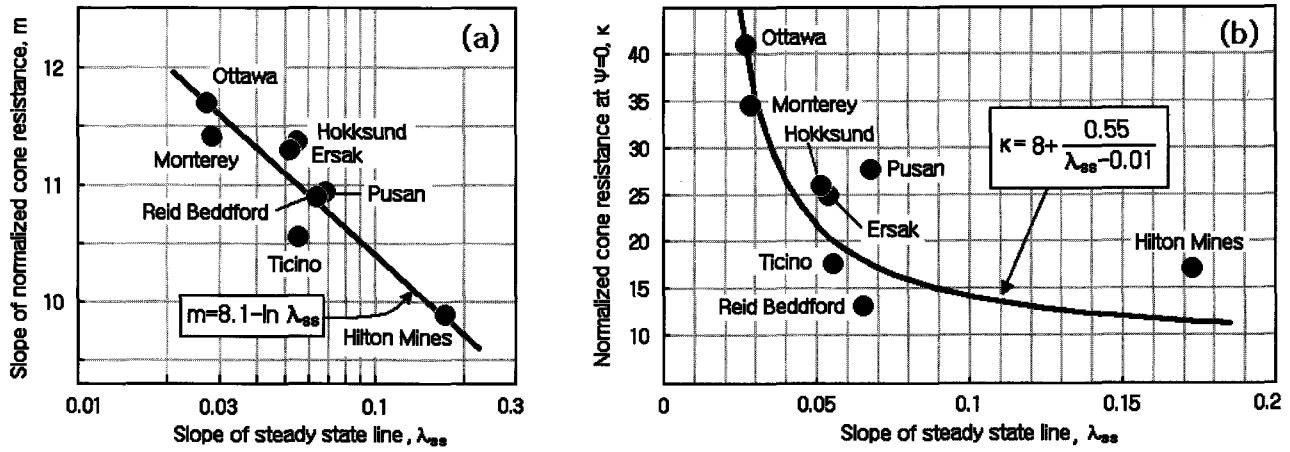

(a) Relationship between m and λ_{ss}

(b) Relationship between κ and λ_{ss}

Fig. 12. Correlation of m and κ with λ_{ss} (after Been et al., 1987)

Figure 12a, while Busan sand shows the largest κ among the soils with similar λ_{ss} in Figure 12b. The reason the κ did not correlate well with the previously published data may be explained by the high strength of quartz sand. Although the compressibility of Busan sand was the second largest of the various sands, the mineralogy or material strength of Busan sand is believed to be large enough to resist grain rupture during cone probe penetration. Therefore, comparatively high cone resistance and κ are likely to be obtained.

4. Conclusions

From a series of CIDC triaxial tests and the cone penetration tests in a calibration chamber, the relationship between the state parameter and normalized cone resistance for Busan sand dredged from the South Sea was investigated and the following conclusions were drawn.

(1) Using the results of the triaxial tests on specimens showing contractive and dilative responses during shear, the critical state line was established and the critical state parameters of Busan sand were determined as $M = 1.39$ ($\phi_{cs} = 34°$), $\Gamma = 1.07$, and $\lambda = 0.068$. It was also observed that the peak friction angle of Busan sand decreased with increasing state parameter with relationship obtained being within the range suggested by Been and Jefferies (1985).

(2) By evaluating the state parameters for the calibration chamber specimens and the corresponding cone resistances normalized with respect to the mean effective normal stress, the relationship between the normalized cone resistance and state parameter for Busan sand was established to be $(q_c - p)/p' = 27.6 \exp(-10.9\Psi)$. It was also shown that this relationship was independent of the stress history when the cone resistance was normalized with respect to the mean effective normal stress.

(3) The slope of the normalized cone resistance, m, and the normalized cone resistance at $\Psi = 0$, κ, for Busan sand were compared with those of various sandy soils by plotting the data in the relation of m and κ with respect to the slope of the steady state line λ_{ss}. The relationship between the m and λ_{ss} of Busan sand showed a good agreement with the result of Been et al. (1987), while Busan sand was found to have the largest κ among the soils with similar λ_{ss}.

Acknowledgement

This paper is supported by the Construction Core Technology Program (C104A1000009-06A0200-00800) under the KICTTEP Grant.

References

1. Been, K., Crooks, J.H.A., Becker, D.E., and Jefferies, M.G. (1986), "The cone penetration test in sands: Part I, State parameter

interpretation", *Géotechnique*, Vol.36, No.2, pp.239-249.
2. Been, K., and Jefferies, M.G. (1985), "A state parameter for sands", *Géotechnique*, Vol.35, No.2, pp.99-112.
3. Been, K., Jefferies, M.G., Crooks, J.H.A., and Rothenburg, L. (1987), "The cone penetration test in sands: Part II, General inference state", *Géotechnique*, Vol.37, No.3, pp.285-299.
4. Been, K., Jefferies, M.G., and Hachey, J. (1991), "The critical state of sands", *Géotechnique*, Vol.42, No.3, pp.365-381.
5. Bolton, M.D. (1986), "The strength and dilatancy of sands", *Géotechnique*, Vol.36, No.1, pp.65-78.
6. Cho, G.C. (2003), "Determination of critical state parameters in sandy soils from standard triaxial testing (I): Review and application", *Journal of Korean Geotechnical society*, Vol.19, No.1, pp.61-75.
7. Cho, G.C. (2003), "Determination of critical state parameters in sandy soils from standard triaxial testing (II): Experiment and recommendation", *Journal of Korean Geotechnical society*, Vol.19, No.1, pp.77-92.
8. Chu, B. (1995), "An experimental examination of the critical state and other similar concepts for granular soils", *Canadian Geotechnical Journal*, Vol.32, pp.1065-1075.
9. DeGregorio, V.B. (1990), "Loading systems, sample preparation, and liquefaction", *Journal of Geotechnical Engineering*, Vol.116, No.5, pp.805-821.
10. Frost, J.D., and Park, J.Y. (2003), "A critical assessment of the moist tamping technique", *Geotechnical Testing Journal*, Vol.26, No.1, pp.57-70.
11. Ishihara, K. (1993), "The Rankine Lecture: Liquefaction and flow failure during earthquakes", *Géotechnique*, Vol.43, No.3, pp.351-415.
12. Jefferies, M.G., and Been, K. (1987), "Note: Use of critical state representations of sand in the method of stress characteristics", *Canadian Geotechnical Journal*, Vol.24, pp.441-446.
13. Luong, M.P. (1980), "Stress-strain aspects of cohesionless soils under cyclic and transient loading", *International Symposium on Soils under Cyclic and Transient Loading*, Swansea, pp.315-324.
14. Poulos, S.J. (1981), "The steady state of deformation", *Journal of Geotechnical Engineering*, Vol.107, No.GT5, pp.553~562.
15. Robertson, P.K., and Campanella, R.G. (1983), "Interpretation of cone penetration tests. Part I: Sand", *Canadian Geotechnical Journal*, Vol.20, pp.718~733.
16. Vaid, Y.P., and Thomas, J. (1995), "Liquefaction and post-liquefaction behavior of sand", *Journal of Geotechnical Engineering*, Vol.121, No.2, pp.163-173.

(received on Jan. 31, 2007, accepted on Mar. 26, 2007)